Control of a Wheelchair using an Adaptive K-Means Clustering of Head Poses

Luis A. Rivera[1] and G. N. DeSouza[2]
ViGIR - Vision-Guided and Intelligent Robotics Lab
ECE Department, University of Missouri
349 Eng. Building West, Columbia, MO, 65211
Email: [1]larmbc@missouri.edu, [2]DeSouzaG@missouri.edu

***Abstract*—Operating a wheelchair is often a difficult task for individuals with severe disabilities. Also, with the progress of the condition, the use of most current robotic assistive technologies becomes less attractive or simply not applicable anymore. In this work, we developed a system that allows a user to operate a wheelchair using only their heads. Our method utilizes an Infrared (IR) depth sensor to capture the user's head pose, while it includes an adaptive component to the detection of that pose. The adaptation, based on a type of *Re-enforcement K-Means* clustering, can accommodate users with limited and changing head mobility – no matter how skewed the head motion may become with the progress of the condition. We tested the system using five test subjects, who simulated 'normal' an 'abnormal' motions of the head. The system worked well in all cases, and all test subjects found the interface quite intuitive.**

***Index Terms*—Head pose, limited mobility, Random Regression Forest, K-means clustering, wheelchair control.**

I. Introduction

Millions of individuals in the U.S. alone experience impaired mobility usually accompanied by limited to no manual dexterity [1], [2], [3], [4]. In spite of the current advances in assistive technologies, those individuals are often unable to effectively interface with computers, cell phones, power wheelchairs, and many other appliances due to: 1) the limitations of these technologies vis-à-vis the specific disabling condition; 2) the inability of the technology to adapt to the disease progression; 3) the fatigue and exertion imposed by prolonged exposures to a single form of technology (i.e. single interface); and 4) the difficulties in adaptation/training and the consequent resistance by patients to move from one technology to the next [5], [6], [7].

Despite all the advances in smart wheelchairs and mobile robot navigation in general [8], [9], [4], [10], [11], little has translated into feasible, robust and cost-effective technology that can truly revolutionize the ability of severely disabled users to fully and independently perform activities of daily living. Indeed, researchers have designed innumerous interfaces for the control of power wheelchair relying, for example: on bio-electrical signals such as EMG, EKG, EEG, etc. [12], [13], [14], [15], [16], [17], [18], [19]; on the configuration of face and head [20], [21], [22], including the use of special hats outfitted with 6-axis gyroscopes [23], [24]; on sitting posture [25]; etc. However, many more different types of interfaces must still be developed in order to allow for greater variety in modality of the interfaces, and consequently minimize fatigue/exertion, minimize down-time due to adaptation, and maximize the effective use of the appliances.

In this work, we propose one such interface. Using a Microsoft Kinect depth sensor and an algorithm based on Random Regression Forests [26] we provide a new approach for controlling power wheelchairs using head poses. We also provide a method of adaptation to the progress of the disabling condition. A K-Means clustering algorithm detects the changes in the range and direction of the head movements and adapts the controls sent to the wheelchair to reflect those changes. The clustering and the associated adaptation are performed using feedback from the sonar sensors, which provides a kind of *re-enforcement* rule that indicates when the driver is not doing so well – e.g. hitting or moving dangerously close to walls.

We tested the system using five individuals, who operated the chair while emulating both *normal* and *abnormal* conditions – i.e. by moving their heads along approximately orthogonal axes and later enforcing changes in those patterns of head motion by limiting and skewing those axes to emulate physical impairments.

Figure 1. High Level System Architecture

II. Background and Related Work

When power wheelchairs were first introduced, it became quite apparent that they would greatly enhance the lives of people with disabilities. Additionally, research began on various methods attempting to control these wheelchairs with means other than a joystick. One such method that has become quite popular among researchers relies on bio-electrical signals from individuals operating the wheelchair. In [18], [19], we employed surface electromyographic signals (sEMG) to take muscle readings on the skin of a user's arm and forehead. In this way, the wheelchair could be controlled by flexing one's hand or eyebrows in various ways to communicate

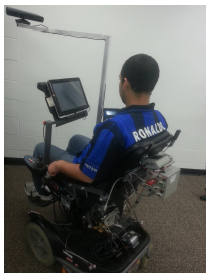

Figure 2. Wheelchair outfitted with an IR depth sensor

predetermined commands to move the chair. One shortcoming of this technique is that it requires extra hardware to collect these signals and, so far, it only allows for four separate commands (Forward, Backward, Left, Right) at a preset speed.

Another method for using electric bio-signals is found in [15], where the authors utilize electrooculography (EOG) to allow a user to use their eyes to control the wheelchair. This is a concept which allowed people to traverse freely without the use of their hands. However, it required the wearing of several sensors on one's face which could be quite cumbersome.

Many diseases such as ASL leave the afflicted individuals with little motor ability below the neck. Additionally, certain spinal cord injuries can also deprive the use of the limbs. In those cases, a person with disability could resort to the use of their head to convey commands to the wheelchair. Though this can be carried out as it was done in [15] – by attaching head sensors – it is more intuitive to utilize a method that does not require complicated attachments (e.g. various self-adhesive electrodes on different points of the head). In both [23] and [24], a system was created to make use of a hat outfitted with a gyroscope. However, only 5 commands were created and achieving more complex driving, such as a gradual arc, became quite difficult.

One way of controlling a wheelchair without placing sensors on a person is by observing the user with a camera. This method was employed in [20], [21], [22]. In [20] for example, the authors used a camera to recognize facial movements like eye closing and opening. In both [21] and [22], a visible light camera was used to gauge the head pose, but only left/right or forward/backward were classified. Additionally, the use of a visible light camera is very sensitive to lighting conditions and may not operate well in dimly lit environments.

In the next section, we explain how our system works and how it manages to adapt, not only to different users, with different levels of disabilities, but also to the progress of the disabling condition. The proposed setup of the system, depicted in Figure 2, can accommodate for a large variety of ranges and directions of motion of the head as it will also be explained later.

III. Proposed System

Our system is based on the K-means clustering method, which is a hard clustering scheme using point representatives and Euclidean distances to measure dissimilarities between vectors and cluster representatives [27]. However, as it will be explained in greater detail next, in order to adapt the clusters over time, we propose a new re-enforcement K-means clustering using sonar sensor information. Many other adaptive and evolving clustering algorithms have been proposed in the literature – e.g. eClustering, Vector Quantization (eVQ), Evolving Local Means (ELM), etc. [28], [29], [30]. While in this paper we do not provide a comparison of these other methods against our new re-enforcement K-means, we believe our solution is sufficiently accurate, adaptable, and simpler, given the characteristics of our problem.

As we mentioned earlier, our method for controlling a wheelchair relies on an IR depth camera to extract head poses. These poses are then used to gauge the user's intention to move the wheelchair. In order to facilitate the estimation of the head pose from a depth image, we utilize a technique created by Fanelli et al in [26]. The technique, called Random Regression Forest (RRF), generates an estimate of the full head pose – i.e. *x, y, z, roll, pitch,* and *yaw*.

A. System Architecture

The software architecture of our system is composed of five modules depicted in Figure 3. In this section, we will describe these modules in more detail.

In fact, the real first step of the algorithm, not depicted in Figure 3, involves the transformation of the 11-bit value returned by the Kinect into actual *(x, y, z)* distances. This process is described in Burrus website[1]. Another step also omitted from the same figure is a threshold filtering that restricts the space where the user head can occupy. This threshold keeps anyone standing around or behind the wheelchair from affecting the results of the head pose estimation.

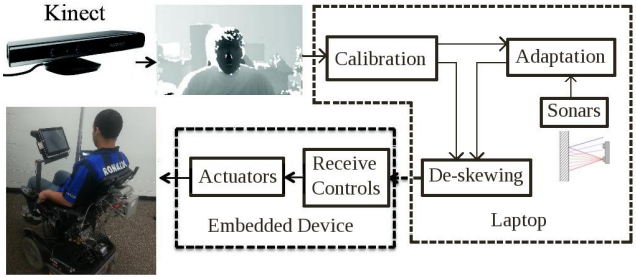

Figure 3. Diagram of Proposed System

1) Calibration: Our system begins by performing a calibration of the head motions to tailor the algorithm to each user. The calibration is quick and simple, and it allows the user to set the coordinates of their control system to the most comfortable configuration. The calibration process starts with instructing the users to orient their heads in a comfortable relaxed position. This position will be later associated with the "Stop" command. The user should remain still for a few seconds, until the system can capture a certain number N of

[1]http://nicolas.burrus.name/index.php/Research/KinectCalibration

head-pose estimates – i.e. sample points containing the *x, y,* and *z,* coordinate of the head as well as its *roll, pitch*, and *yaw* orientations. Next, the users are instructed to orient their heads to the "Left", "Right", "Forward", and "Backward" poses – each of these reference poses are held until the system can again capture N samples returned by the RRF algorithm. The samples are clustered and the centers of the clusters become the representatives of their classes. These centers will be used to define a reference coordinate frame for adjusting future head poses for each user. Furthermore, it is assumed that orienting the head in a pose similar to the cluster centers implies a desire by the driver to move at maximum speed. For instance, orienting the head as in the "Forward" cluster center should be translated into moving the wheelchair forward at maximum speed. Similarly, orienting the head as in the "Left" cluster center should translate into turning the wheelchair in place, to the left, also at the maximum rotational speed. Orienting the head between "Stop" and one of the other four poses would lead to a speed proportional to the distance to that corresponding cluster center.

The training samples and the cluster centers are stored by the system and will be used later, during the adaptation. Once the initial calibration is completed, the user can start using the system to actually control the wheelchair. Figure 4 shows the calibration results for three of the five different users used in our tests.

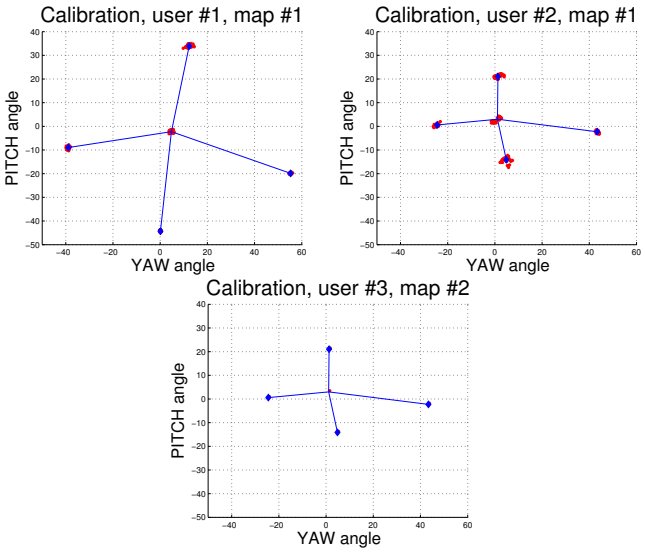

Figure 4. Calibration results for users #1 to #3. The calibration samples are displayed in red; the cluster centers are shown in blue with the reference coordinate frames also in blue. The angles are in degrees.

2) De-skewing: Before we explain the other modules of the system, let us skip to the last module. At this point, the system is constantly generating new estimates of *yaw* and *pitch* based on the head-pose outputs from the previous modules. Also, each one of these head poses must be translated into commands for the wheelchair – e.g. move forward, turn, etc. However, since these head poses may be skewed by the limited motion imposed by the disabling condition, these head poses must be first de-skewed. The idea behind this de-skewing process is that the five cluster centers obtained during calibration – i.e. "Stop", "Left", "Right", "Forward", and "Backward" – will now form a coordinate system, with the "Stop" cluster center as its origin. This coordinate system is not necessarily orthogonal, as shown in Figure 5 by the red axes. So, before any head pose sample can be mapped into a command to the chair, its projections onto the reference coordinate system must be found.

This process is quite simple. The only slight complication is due to the fact that the ranges of motion provided during calibration may not be the same in all four directions of the head motion. Another small complication comes from the center of the cluster "Stop", which despite being regarded as the origin of the reference coordinate system, it may have coordinate $C_{"Stop"} = (yaw_{"Stop"} \neq 0,\ pitch_{"Stop"} \neq 0)$.

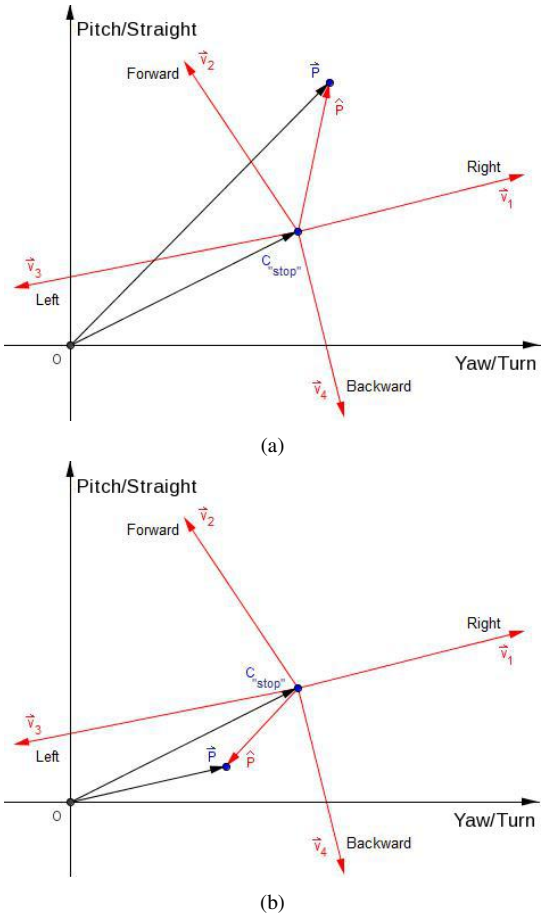

Figure 5. Two examples of the de-skewing process for head poses: (a) first and (b) third quadrants.

Graphically, the de-skewing process is illustrated in Figure 5a and b. Mathematically, the same process is as follows. A head-pose sample $\overrightarrow{P} = (yaw,\ pitch)$ must be translated to the *skewed,* reference coordinate system. That is represented by the point $\hat{P} = \overrightarrow{P} - C_{"Stop"} = (yaw - yaw_{"Stop"},\ pitch - pitch_{"Stop"})$. Next, this point $\hat{P}$, which in our first example

(Figure 5a lies on the first quadrant, must be projected onto a pair of axes describing that quadrant – in this case, the vectors $\overrightarrow{v_1}$ and $\overrightarrow{v_2}$, since, again, $\hat{P}$ lies on the first quadrant, which is defined by the "Forward" axis $\overrightarrow{v_1}$ and the "Right" axis $\overrightarrow{v_2}$. Finally, the projections of $\hat{P}$ can be expressed as:

$$\overrightarrow{P} = \alpha_1 \overrightarrow{v_1} + \alpha_2 \overrightarrow{v_2}$$

Where α_1 and α_2 are the actual projections. In matrix form, we have

$$\overrightarrow{P} = VA$$

where $V = \begin{bmatrix} \overrightarrow{v_1} & \overrightarrow{v_2} \end{bmatrix}$, with $\overrightarrow{v_1}$, $\overrightarrow{v_2}$ as column vectors, and $A = \begin{bmatrix} \alpha_1 \\ \alpha_2 \end{bmatrix}$. Since $\overrightarrow{v_1}$, $\overrightarrow{v_2}$ are linearly independent, it follows that V^{-1} exists, and we can obtain A as:

$$A = V^{-1}\overrightarrow{P}$$

Since the projections α_1 and α_2 can be regarded as the *contributions* of the head pose in the "Right" and "Forward" directions, the rotational velocity and the linear velocity of the wheelchair are, respectively:

$$RotVel = -\alpha_1 MaxRotSpeed$$
$$LinVel = \alpha_2 MaxLinSpeed$$

The negative sign for the rotational velocity is just to keep the convention of negative rotational velocities when rotating to the right (clockwise).

As we mentioned above, the ranges of head motion are not necessarily the same in all four directions obtained during calibration. Therefore, the quadrant where $\hat{P}$ lies is important in determining which of the four axes to use – i.e. $\overrightarrow{v_1}$, $\overrightarrow{v_2}$, $\overrightarrow{v_3}$ or $\overrightarrow{v_4}$. In Figure 5b, we illustrate this condition by considering a case where $\hat{P}$ lies on the third quadrant, instead of the first quadrant as in the previous case. In that case, all the discussion above still holds, as long as we replace $\overrightarrow{v_1}$ and $\overrightarrow{v_2}$ by $\overrightarrow{v_3}$ and $\overrightarrow{v_4}$ – i.e. the vectors that describe the third quadrant.

As final remarks, we should mention two things: first, the quadrant to which $\overrightarrow{P}$ belongs does not, by itself, determines the quadrant to which $\hat{P}$ belongs, and yet, it is the latter rather than the former that determines which set of basis vectors, $\overrightarrow{v_1}$, $\overrightarrow{v_2}$, $\overrightarrow{v_3}$ or $\overrightarrow{v_4}$ to use; and second, that if the coefficients α_1 and α_2 are close to zero (less than 10% of the full motion), the actual velocities are set to zero. This allows the wheelchair to remain stationary even if the users move their heads slightly off the "Stop" position.

3) Adaptation: Over short periods of time, users may become fatigued and they may need to reposition their bodies on the wheelchair. Also, over long periods of time, the disease may progress, imposing greater limitations on the ranges and angles of the head motions. In either cases, the head motions start deviating from the calibrated poses. In order to avoid forcing the user to re-calibrate the system, we included an adaptation algorithm based on K-means. For this adaptation, which is one of the main contributions of this work, we use sonar sensors as a source of re-enforcement to be applied on top of the K-means clustering. These ideas are explained in greater details in the next two subsections.

a) Re-enforced K-Means: The assumption here is that any deviation from the calibrated head poses should lead to a "*bad driving*" of the wheelchair. That is, if the user is trying to move forward along a hallway, but due to fatigue or any other sudden or progressive change in his head movements he can no longer position his head as in the calibrated "Forward" pose, the wheelchair will likely start to turn, even if so slightly. That will cause the wheelchair to move into obstacles or even the wall. If we could detect this situation, we could use this information to adapt the calibrated head poses to these new conditions.

One easy way of detecting this *"bad driving"* situation is by the use of sonar sensors. In our case, we use sonars that can detect obstacles up to 5 meters in 16 different directions. These directions of the sonar sensors are presented in Figure 6a). Also, from the sensor readings and the current motion command sent to the wheelchair, the system can infer if there should be an adaptation of the head pose clusters. This idea is depicted in Figure 6b), where the user orients his head slightly deviated to the right from the calibrated "Forward" position. If a sensor detects an obstacle/wall to the right of the wheelchair, the situation is flagged as a *"bad driving"*, indicating that an adaptation of the clusters must be performed.

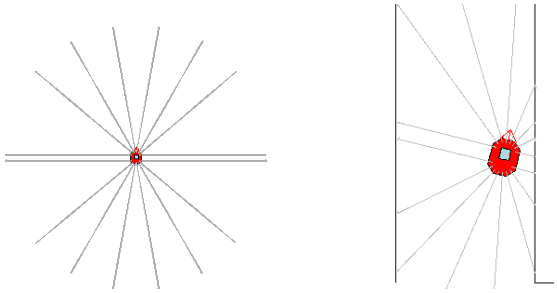

(a) Available directions of the sonar sensors (16)

(b) Wheelchair moving towards an obstacle or wall

Figure 6. Situation when the commanded direction of motion overlaps with some of the sonar sensors.

In fact, the adaptation occurs at all times, but the head poses are handled differently, depending on the need or not to re-enforce the learning due to a *"bad driving"* behavior. When no obstacles are detected in the direction of motion, the samples are considered regular, and they are eliminated from the dataset used for adaptation. On the other hand, if the system detects a *"bad driving"* behavior, the corresponding head-pose sample is stored and used for clustering. If the proximity to the obstacle is alarming, a weight of 2 is assigned to this head-pose sample. If the proximity is medium, a weight of 1 is assigned.

It should go without saying that new samples lead to new cluster centers, which leads to new axes $\overrightarrow{v_1}$, $\overrightarrow{v_2}$, $\overrightarrow{v_3}$ and $\overrightarrow{v_4}$ to be calculated, which in turn leads to completely different commands to the wheelchair – and an adaptation to the changes in head motions and ranges is achieved.

b) Actual Clusters and Clustering: During the calibration process described in III-A1, $5 \times N$ samples are stored

with the corresponding labels – "Stop", "Right", "Forward", "Left" and "Backward". After that, four additional clusters are artificially created: "ForwardRight" ,"ForwardLeft", "BackwardLeft" and "BackwardRight". The reason for creating these artificial clusters will be explained below. In the meantime, we should say that these clusters are obtained as a combination of the centers of the other clusters. For instance, the "BackwardLeft" cluster is defined as:

$$BL = O + \frac{\sqrt{2}}{2}\left(\overrightarrow{OC_B} + \overrightarrow{OC_L}\right)$$

where O is the origin, or the center of the "Stop" cluster, and C_B and C_L are the centers of the "Backward" and "Left" clusters, respectively. The factor $\frac{\sqrt{2}}{2}$ was chosen to approximately preserve the ranges of the two axes involved – i.e. to pick a point in the middle of a circular arc going from C_L to C_B instead of a mid-point between the two. The remaining diagonal clusters are obtained in a similar fashion, and N copies for each of these artificially created centers are stored in the respective clusters.

In order to prevent unnecessary clustering with insufficient number of samples, the clustering only occurs once the system collects T new samples. These new samples are then mixed together with all the previously stored samples from all 9 classes. Samples with a weight different from 0 are stored multiple times equal to the weight itself. Then, the K-means clustering algorithm is run to obtain new clusters and cluster centers. This differentiated weighting of samples allows for *"bad driving"* behaviors to quickly modify the cluster centers. At the same time, the reason for the system to preserve previous samples from all 9 classes in addition to the new weighted samples is to avoid abrupt changes in behaviors. Also, after the adaptation, the system preserves only the newest N samples for each of the 9 classes. This will ensure that no cluster will *disappear* due to the lack of *"bad driving"* behavior in the direction associated with that cluster.

Finally, the reason to create the artificial clusters is to prevent the original four clusters from merging together. During our experiments, we noticed that users produce many samples in the diagonal between two of the original clusters. That is a natural consequence of the driving, which involves constant diagonal motions instead of sharp, 90-degree, turns. If we did not have these artificially created clusters, the system would not be able to determine whether the pattern of head motions was changing or the user was simply *cutting corners* and the four original clusters would simply disappear.

IV. Experimental Results

In this section, we present the results from the experiments performed to validate the system. Our goal here is to demonstrate the flexibility of the system in adapting to different users and to changing conditions of a specific user. While the system presented here was tested using the MobileSim simulator, a video showing its operation on a real wheelchair is available at http://tinyurl.com/cgpl4a5

In total, five test subjects – users #1 to #5 – participated in a set of experiments using three different maps. For the first experiment, we asked users #1 to #3 to drive the wheelchair using maps #1 and later map #2. In the second experiment, user #4 was asked to perform a head movement with very skewed axes and limited ranges. The goal was to simulate a person with an impediment to move his head orthogonally. Finally, in the third test, user #5 was asked to change the pattern of head motion and test the adaptability of the system to such changes.

For all three experiments described next, the cluster size, N, was set to fifty, and the number of samples T needed to trigger an adaptation was also set to fifty.

A. Testing under normal conditions

For the first experiment, we asked users #1 to #3 to complete the trajectory with no large limitations on the ranges or directions of the head motions. The idea was to simulate a person with minor disabilities. The users performed the initial calibration (Figure 4) and then drove a wheelchair through map #1. They were asked to make often stops in the middle of the map, and also to go backwards along at least one stretch of the map. Then, they were asked to drive through the first map two more times. After running the experiment using the first map, the users were asked to move to a second map. This time, there was no calibration and the system relied on the previously stored clusters. The users completed the second map three times as well.

Figure 7 depicts the evolution of the cluster centers over time, as the users drove through the maps. Due to space limitations of this paper, the figure presents users #1 and #2 for map #1, and user #3 for map #2. In Figure 8 we present the corresponding maps with the trajectories followed by those users over the three trials. Finally, Figure 9 shows the sample points collected for the first trial over the maps in Figure 8. Regular samples, or samples of *"good driving"* are represented in light blue. Samples in dark blue are those to which a weight of 1 was assigned – those are the *"bad driving"* behaviors that led to medium proximity to an obstacle or wall. Finally, samples in red are those assigned a weight of 2, or with alarming proximity. Notice that if there were not many *"bad driving"* situations, the system would take longer to trigger an adaptation. On the other hand, constant *"bad driving"* situations would lead to more often adaptation. Typically, the system triggered an adaptation any time between 30 and 120 seconds, depending on the user. User #1 caused almost no adaptations throughout the maps.

All users successfully completed the courses on both maps. As it can be observed from Figures 8 and 9, the first user moved his head in the most consistent way: the head pose samples were very close together. At the same time, we observe a larger spread in the data for users #2 and #3. Also, in Figure 7 for user #1, the variation of the centers was very small, while for users #2 and #3 the centers shifted considerably more. The first subject produced mostly pure movements: forward, backward, left or right. Only a small portion of his samples were categorized as *"bad driving"* – shown in dark blue or red in Figure 9. Users #2 and #3, on the

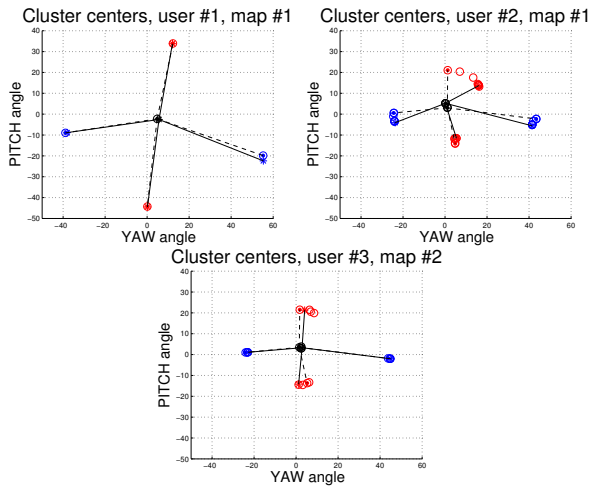

Figure 7. Evolution of the cluster centers over time for users #1 and #2 (on map #1) and user #3 (on map #2). A dot represents the initial position and a "*" represents the final position of the cluster centers. The circles represent intermediate positions. The "Stop" pose is in black, the "Forward" and "Backward" centers are in red, while the "Left" and "Right" centers are in blue. The initial axes are shown as dashed lines, while the final axes are shown as continuous lines. The angles are in degrees.

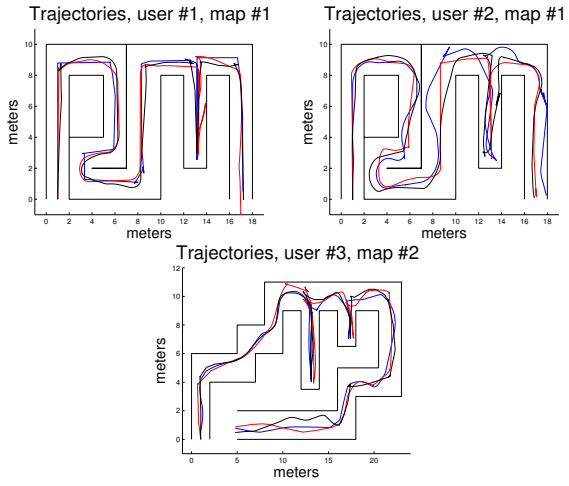

Figure 8. Trajectories followed by users #1 and #2 on the first map, and by user #3 on the second map.

other hand, drove a lot less consistently. They went closer to the walls more often, and they frequently moved their heads "diagonally". The sample points in the second and third plots of Figure 9 are more evenly distributed in the *yaw-pitch* space. Also, a higher fraction of the points were assigned a weight of 1 (dark blue) or even 2 (red). Consequently, the cluster centers were updated on many more occasions than for user #1.

B. Tolerance of the system to initial calibration of the axes

We asked a fourth user to calibrate the system with highly skewed head poses. The goal was to simulate a person with difficulty to move his head orthogonally. The results for driving through map #1 are shown in Figure 10. Despite being a very skewed reference frame, the limitations in range

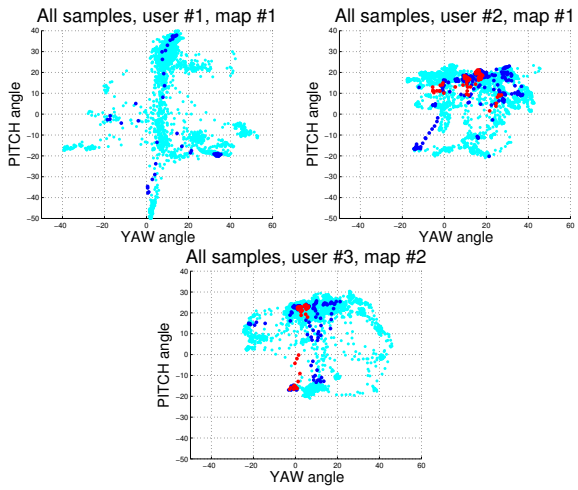

Figure 9. Head-pose samples collected when users #1 to #3 drove through maps #1 and #2. Regular samples are plotted in light blue; samples with weight 1 in dark blue; and samples with a weight of 2 in red.

of motion still led to clusters with much smaller dispersion. Moreover, the user was able to successfully complete the course in all three trials. Also, it can be noticed that a small number of points were assigned a weight different from zero. Therefore, the reference frame was only updated a few times. The only cluster that showed more noticeable change was the "Forward" cluster.

Next, the user was asked to re-calibrate the system, using a different set of head poses and drive through map #2. Figure 11 shows the results for this experiment. As before, even though the axes were highly skewed, the subject was able to complete the second course without problems, and for all trials. Here, we notice that the "Down" and "Right" clusters were the ones that changed over time.

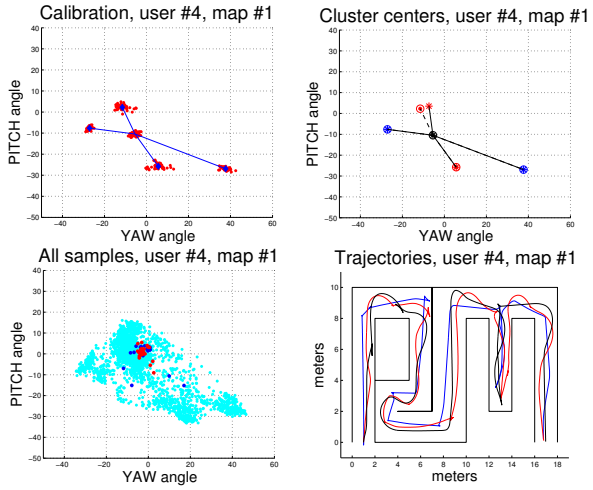

Figure 10. Test of highly skewed axes of head pose: first plot shows the initial calibration; the second plot, the evolution of the cluster centers; head-pose samples are shown in the third plot; and the trajectories followed by user #4 on map #1 are shown in the last plot.

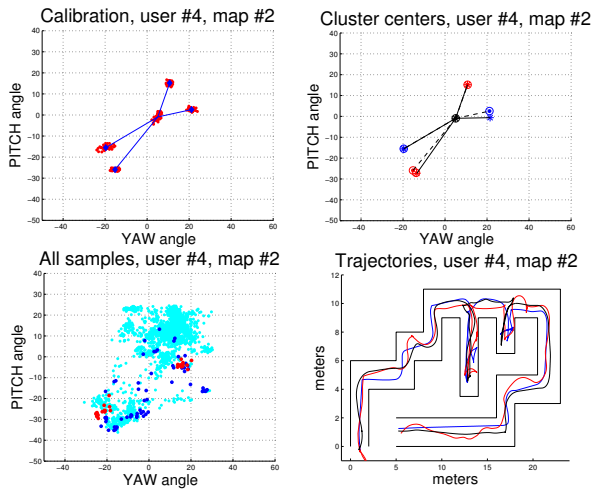

Figure 11. Another test of highly skewed axes of head pose using map #2. Once again, each plot in sequence shows: the initial calibration; the evolution of the cluster centers; head-pose samples; and the trajectories followed.

C. Further Test of Adaptability

The last test presented here aimed at demonstrating the effectiveness of the adaptation of the proposed system. Two similar trials were performed. In both cases, user #5 was asked to go through map #3, which consists of a long corridor. The user started at the center, and then intentionally tilted his head towards the wall until the wheelchair actually hit the wall. Then, he was asked to back up, reposition the wheelchair at the center of the hallway and repeat the process until the end of the hallway. Finally, the user was asked to move back to the beginning of the corridor, and start moving up once again – this time keeping approximately the same tilted position of the head that led the wheelchair to hit the wall in the first and second runs.

Figures 12 and 13 show the results for the two trials of this experiment. In the first trial, the user leaned to the right wall and in the second the user leaned to the left. The trajectories followed by the wheelchair show how it started straight and then it quickly moved towards the wall. After backing up for the first time and repositioning the wheelchair in the center of the corridor, the trajectories continued towards the end. This time, the wheelchair still leaned towards the wall, but at a much smaller angle. The evolution of the cluster centers, also depicted in Figures 12 and 13, demonstrates how the "Forward" cluster adapted by shifting to the right and left, depending on the trial. This is consistent with all the weighted samples shown in the third part of Figures 12 and 13. In fact, because of this same adaptation of the "Forward" cluster, the tilted head pose had already led to a straighter line in the second run when compared to the first run – see the first part of Figures 12 and 13.

V. Conclusions and Future Work

We presented a system for controlling a wheelchair using only head poses. The results of our experiments, with five users, and various trials show the flexibility of the system and its ability to adapt to different users – whether they present limitations in their head motions or not. Driving the wheelchair with the head was intuitive, as demonstrated in the video and in the simulations presented here. The system was tested using a variety of ranges of head motion and for different initial calibrations. No matter how the system was calibrated the users were still able to navigate the course with ease. Throughout all the trials, no user ever collided with the walls of the map, except when asked to do so.

The adaptability and flexibility of the system can be attributed to the proposed *Re-enforcement K-means* algorithm

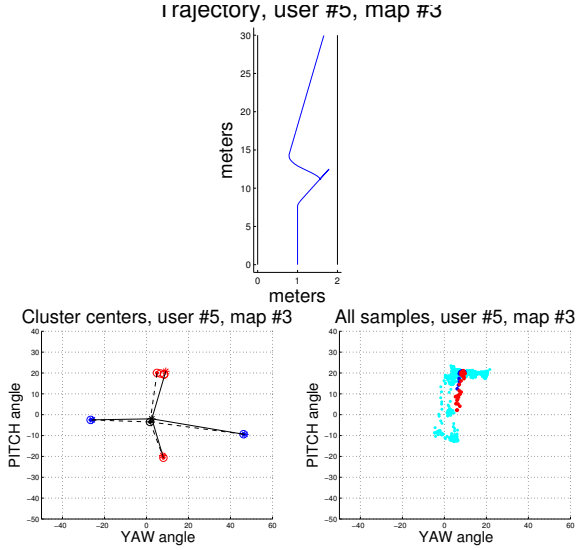

Figure 12. Trajectory followed by user #5 (going to the right wall), evolution of the cluster centers and all the sample points. Notice that the weighted samples are in the diagonal to the right. The cluster center corresponding to forward moved toward that position.

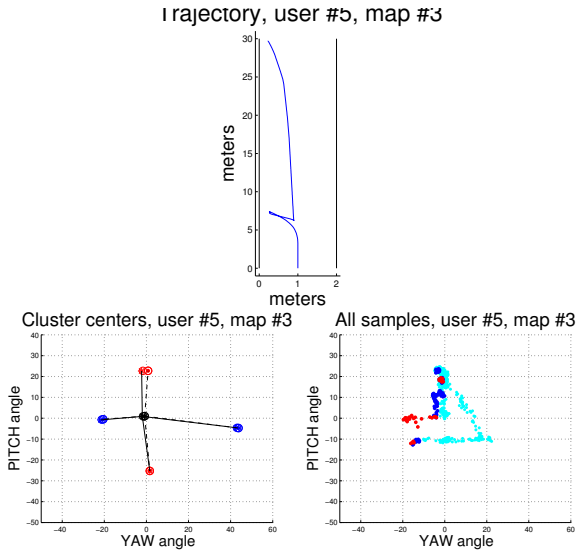

Figure 13. Trajectory followed by user #5 (going to the left wall), evolution of the cluster centers and all the sample points. Notice that the weighted samples are to the left. The cluster center corresponding to forward shifted a bit to the left.

for clustering. The algorithm takes cues from the driving behavior of the user and feeds back *"bad"* behaviors to fix the clustering and achieve better driving.

One of the users faced difficulty in having her head tracked by the system. That person uses a scarf around her head, and the system was not able to locate her head. Since this research is not on head tracking, we omitted this result. However, in the future, we intend to use Active Appearance Models [31], [32], [33] to help improve the head pose estimations.

Further tests must be carried out, specially with persons with true disabling conditions. Also, further investigation on the parameters chosen for the system, such as cluster size, weights for *"bad driving"*, threshold for triggering the adaption, and the ranges for maximum speeds should be considered. Finally, the use of other environmental cues could be used to guide the adaptation, such as eye gaze, involuntary collision with moving obstacles – which should not be regarded as *"bad driving"* – etc.

REFERENCES

[1] E. Department, "Notice of final long-range plan for fiscal years 2005-2009," in *71 FR 8165*. Federal Register DOCID:fr15fe06-165, National Institute on Disability and Rehabilitation Research, Education Department, February 15, 2006, pp. 8165–8200.

[2] S. P. Parikh, V. G. Jr, V. Kumar, and J. O. Jr, "Integrating human inputs with autonomous behaviors on an intelligent wheelchair platform," *IEEE Intelligent Systems Magazine*, pp. 33–41, March/April 2007.

[3] V. Kumar, T. Rahman, and V. Krovi, "Assistive devices for people with motor disabilities. wiley encyclopedia for electrical and electronic engineers," 1997.

[4] R. C. Simpson, "How many people would benefit from a smart wheelchair?" *Journal of Rehabilitation Research and Development*, vol. 45, no. 1, pp. 53–72, 2008.

[5] M. Kohler, C. F. Clarenbach, L. Boni, T. Brack, E. W. Russi, and K. E. Bloch, "Quality of life physical disability and respiratory impairment in duchenne muscular dystrophy," *American Journal of Respiratory and Critical Care Medicine*, vol. 172, no. 8, pp. 1032–6, 2005.

[6] N. Pellegrinia, B. Guillona, H. Prigenta, M. Pellegrinia, D. Orlikovskia, J.-C. Raphaela, and F. Lofasoa, "Optimization of power wheelchair control for patients with severe duchenne muscular dystrophy," *Neuromuscular Disorders*, vol. 14, no. 5, pp. 297–300, 2004.

[7] M. Trail, N. Nelson, J. N. Van, S. H. Appel, and E. C. Lai, "Wheelchair use by patients with amyotrophic lateral sclerosis: a survey of user characteristics and selection preferences," *Archives of Physical Medicine and Rehabilitation*, vol. 82, no. 1, pp. 98–102, 2001.

[8] G. N. DeSouza and A. C. Kak, "Vision for mobile robot navigation: A survey," *IEEE Transactions on Pattern Analysis and Machine Intelligence*, vol. 24, no. 2, pp. 237–267, 2002.

[9] R. C. Simpson, "Smart wheelchairs: A literature review." *Journal of Rehabilitation Research and Development*, vol. 42, no. 4, pp. 423–436, 2005. [Online]. Available: http://view.ncbi.nlm.nih.gov/pubmed/16320139

[10] G. Bourhis and M. Sahnoun, "Assisted control mode for a smart wheelchair," *ICORR 2007 IEEE 10th International Conference on Rehabilitation Robotics*, pp. 158–163, June 2007.

[11] G. Bourhis and Y. Agostini, "Man-machine cooperation for the control of an intelligent powered wheelchair," *Journal of Intelligent and Robotic Systems*, vol. 22, no. 3-4, pp. 269–287, 1998.

[12] M. Khezri and M. Jahed, "A novel approach to recognize hand movements via sEMG patterns," in *29th Annual International Conference of the IEEE EMBS*, Aug. 2007, pp. 4907–4910.

[13] ——, "Real-time intelligent pattern recognition algorithm for surface EMG signals," *BioMedical Engineering OnLine*, vol. 6, no. 1, p. 45, 2007.

[14] G. Shuman, "Using forearm electromyograms to classify hand gestures," in *IEEE International conference on Bioinformatics and Biomedicine*, 2009, pp. 261–264.

[15] R. Barea, L. Boquete, M. Mazo, and E. Lopez, "System for assisted mobility using eye movements based on electrooculography," *Neural Systems and Rehabilitation Engineering, IEEE Transactions on*, vol. 10, no. 4, pp. 209–218, dec. 2002.

[16] M. R. Ahsan, M. I. Ibrahimy, and O. O. Khalifa, "Advances in electromyogram signal classification to improve the quality of life for the disabled and aged people," *Journal of Computer Science*, vol. 7, no. 6, pp. 706–715, 2010.

[17] B. Rebsamen, E. Burdet, C. Guan, H. Zhang, C. L. Teo, Q. Zeng, C. Laugier, and M. H. Ang Jr., "Controlling a wheelchair indoors using thought," *Intelligent Systems, IEEE*, vol. 22, no. 2, pp. 18–24, march-april 2007.

[18] L. A. Rivera and G. N. DeSouza, "Recognizing hand movements from a single sEMG sensor using guided under-determined source signal separation," in *12th IEEE International Conference on Rehabilitation Robotics*, Jun 2011, pp. 450–455, eTH Zurich, Switzerland.

[19] ——, "A power wheelchair controlled using hand gestures, a single sEMG sensor, and guided under-determined source signal separation," in *IEEE International Conference on Biomedical Robotics and Biomechatronics*, June 2012, july 24-28.

[20] L. Wei, H. Hu, T. Lu, and K. Yuan, "Evaluating the performance of a face movement based wheelchair control interface in an indoor environment," in *Robotics and Biomimetics (ROBIO), 2010 IEEE International Conference on*, dec. 2010, pp. 387–392.

[21] C. Bauckhage, T. Kaster, A. Rotenstein, and J. Tsotsos, "Fast learning for customizable head pose recognition in robotic wheelchair control," in *Automatic Face and Gesture Recognition, 2006. FGR 2006. 7th International Conference on*, april 2006, pp. 311–316.

[22] Z. fang Hu, L. Li, Y. Luo, Y. Zhang, and X. Wei, "A novel intelligent wheelchair control approach based on head gesture recognition," in *Computer Application and System Modeling (ICCASM), 2010 International Conference on*, vol. 6, oct. 2010, pp. 159–163.

[23] D. Craig and H. Nguyen, "Wireless real-time head movement system using a personal digital assistant (pda) for control of a power wheelchair," in *Engineering in Medicine and Biology Society, 2005. IEEE-EMBS 2005. 27th Annual International Conference of the*, sept. 2005, pp. 6235–6238.

[24] L. King, H. Nguyen, and P. Taylor, "Hands-free head-movement gesture recognition using artificial neural networks and the magnified gradient function," in *Engineering in Medicine and Biology Society, 2005. IEEE-EMBS 2005. 27th Annual International Conference of the*, jan. 2005, pp. 2063–2066.

[25] J. Fan, S. Jia, X. Li, W. Lu, J. Sheng, L. Gao, and J. Yan, "Motion control of intelligent wheelchair based on sitting postures," in *Mechatronics and Automation (ICMA), 2011 International Conference on*, aug. 2011, pp. 301–306.

[26] G. Fanelli, T. Weise, J. Gall, and L. V. Gool, "Real time head pose estimation from consumer depth cameras," in *33rd Annual Symposium of the German Association for Pattern Recognition (DAGM'11)*, September 2011.

[27] S. Theodoridis and K. Koutroumbas, *Pattern Recognition*. Academic Press, 2006.

[28] B.-R. Dai, J.-W. Huang, M.-Y. Yeh, and M.-S. Chen, "Adaptive clustering for multiple evolving streams," *Knowledge and Data Engineering, IEEE Transactions on*, vol. 18, no. 9, pp. 1166 –1180, sept. 2006.

[29] E. Lughofer, "Dynamic evolving cluster models using on-line split-and-merge operations," in *Machine Learning and Applications and Workshops (ICMLA), 2011 10th International Conference on*, vol. 2, dec. 2011, pp. 20 –26.

[30] R. Baruah and P. Angelov, "Evolving local means method for clustering of streaming data," in *Fuzzy Systems (FUZZ-IEEE), 2012 IEEE International Conference on*, june 2012, pp. 1 –8.

[31] P. Mittrapiyanuruk and G. N. DeSouza , "Tracking 3D pose of rigid objects using inverse compositional active appearance models," *Journal of Knowledge-based and Intelligent Engineering Systems*, vol. 14, no. 4, pp. 229–239, Dec 2010, dOI 10.3233/KES-2010-0204.

[32] P. Mittrapiyanuruk, G. N. DeSouza, and A. C. Kak, "Accurate 3D tracking of rigid objects with occlusion using active appearance models," in *Proceedings of 2005 IEEE Motion*, vol. 2, January 2005, pp. 90–95, breckenridge, CO, USA.

[33] ——, "Calculating the 3D-pose of rigid objects using active appearance models," in *Proceedings of 2004 IEEE International Conference on Robotics and Automation*, April 2004, pp. 5147–5152, new Orleans, USA.